Automotive Engineering

Ludomir J. Jankowski, Ph.D. Eng.

Testing of vehicle elements and assemblies

Photoelastic investigation of the towing hitch model

Project co-financed by European Union within European Social Fund

Introduction

Applications of photoelasticity are divided into classes according to the geometric form of the object analyzed. For plane objects, especially those loaded in-plane, the two-dimensional stress state appears and plane models of the object are used. If the object is not plane often more complex (three-dimensional) stress state is generated. For such a case the three-dimensional model of the object must be used (fig. 1).

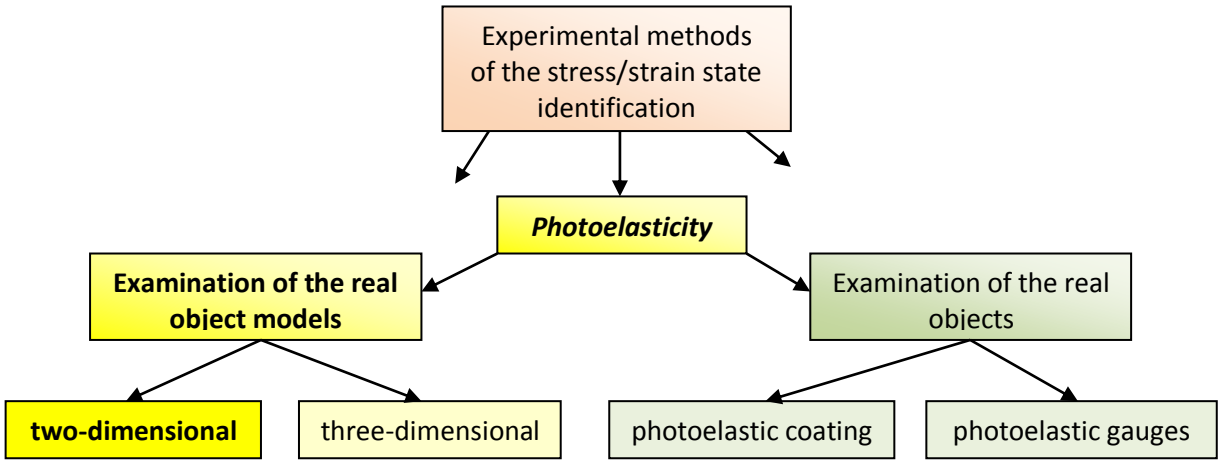

Fig. 1 Classes of the photoelastic techniques

Both two- and three-dimensional applications of photoelasticity are used above all in the early stages of the design process. It is much more favourable to verify design assumptions and modify the geometry of the object examining the less expensive model. Below, the conventional two-dimensional photoelastic analysis is described.

Fundamentals of the two-dimensional model analysis

All the photoelastic techniques are based on two optical phenomena: ***birefringence*** (double refraction) induced by load/strains in transparent materials (glass, epoxy resin, polycarbonate, urethane rubber) and ***light polarization*** generated in polariscopes. In classical applications of the two-dimensional photoelasticity transmission scheme of the light propagation in plane model is used.

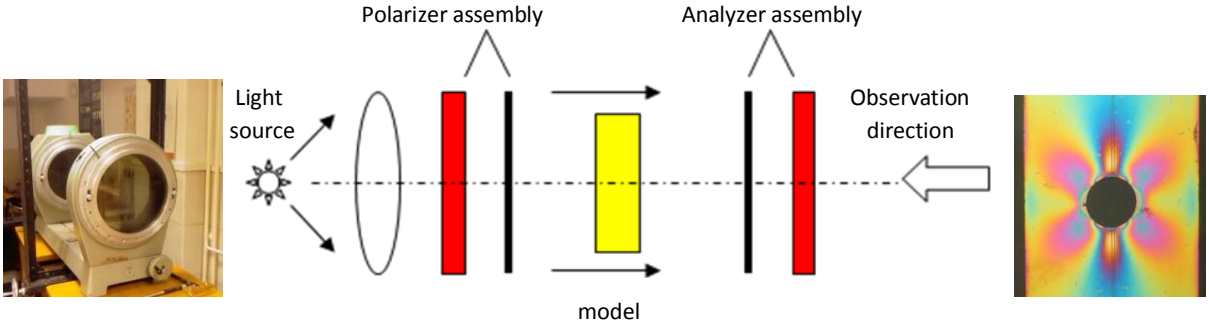

Fig. 1 Scheme of the transmission polariscope

Fig. 2 Transmission polariscope (Carl Zeiss – Jena) Ø 300, white and monochromatic (sodium) light, plane and circular polarization

For efficient photoelastic measurements a full-field registration of the isoclinic and isochromatic patterns (full- and half-order) is the basic requirement for polariscopes. The possibility of the goniometric compensation of the isochromatic fringe order is needed. The polariscope presented above (fig.2) has all these features.

The photoelastic effect in the model is caused by alternately constructive and destructive interference between the light rays which have undergone the relative retardation (phase shift) in the stressed model's material. The observed fringes are proportional to the difference between the principal strains in the model or shear strain:

$$(\varepsilon_1 - \varepsilon_2) = \frac{N f_\varepsilon}{t} \qquad \gamma_{xy} = \frac{N}{2t} f_\varepsilon \tag{1}$$

where f_ε is called strain material fringe value, index *1* and *2* denote principal directions of the strains/stresses, t - is model thickness. Practically, all photoelastic materials presently applied have a high limit of the linear relation of the $\sigma - \varepsilon$ characteristic. Based on this fact and taking in to the consideration that engineers, especially designers, often work with stress relations rather than strain, the equations (1) can be transformed according to the Hook's law. For mechanically isotropic (optically anisotropic under loading) materials in the biaxial stress state, the relationships between strains and stresses are expressed as follows:

$$\sigma_1 = \frac{E}{(1-\nu^2)}(\varepsilon_1 + \nu\varepsilon_2); \qquad \sigma_2 = \frac{E}{(1-\nu^2)}(\varepsilon_2 + \nu\varepsilon_1); \tag{2}$$

$$(\sigma_1 - \sigma_2) = \frac{E}{(1+\nu)}(\varepsilon_1 - \varepsilon_2) = \frac{E}{(1+\nu)}\frac{N f_\varepsilon}{t} = \frac{N f_\sigma}{t} \tag{3}$$

where E is elastic (Young's) modulus of the model material, ν – Poisson's ratio of this material.
The maximum shear stress τ_{max} is expressed by:

$$\tau_{max} = \frac{E}{(1+\nu)}\frac{N f_\varepsilon}{2t} = \frac{N f_\sigma}{2t} \tag{4}$$

Knowing at the point the two photoelastic parameters, i.e. isochromatic fringe order *N* and isoclinic parameter *α,* the difference of the normal stresses and shear stress can be calculated using formulas:

$$\left(\sigma_x - \sigma_y\right) = \frac{N f_\sigma}{t}\cos 2\alpha$$
$$\tau_{xy} = \frac{N f_\sigma}{2t}\sin 2\alpha \qquad (5)$$

The principal stress directions must be measured with reference to an established line, axis or plane. In most cases the reference is a horizontal line or an axis of symmetry of the tested model. The information about those directions are defined by black lines, so-called isoclinics, observed in a plane-polarized light traversing a photoelastic model. At every point on an isoclinic with parameter *α*, the directions of principal stresses are parallel to the direction of polarization of the analyzer and the polarizer. Thus, the measurement of the principal stress directions at any point is accomplished by the rotation of the analyzer and the polarizer together (polarizing filters must be coupled) until a black isoclinic line appears at the point. For this angle of the rotation the reading of the parameter *α* is made.

When the principal stress directions must be determined over the tested area, the isoclinics for the determined parameters *α* (for example α = 0°; α = 15° ...) α are usually recorded by photography (fig. 3).

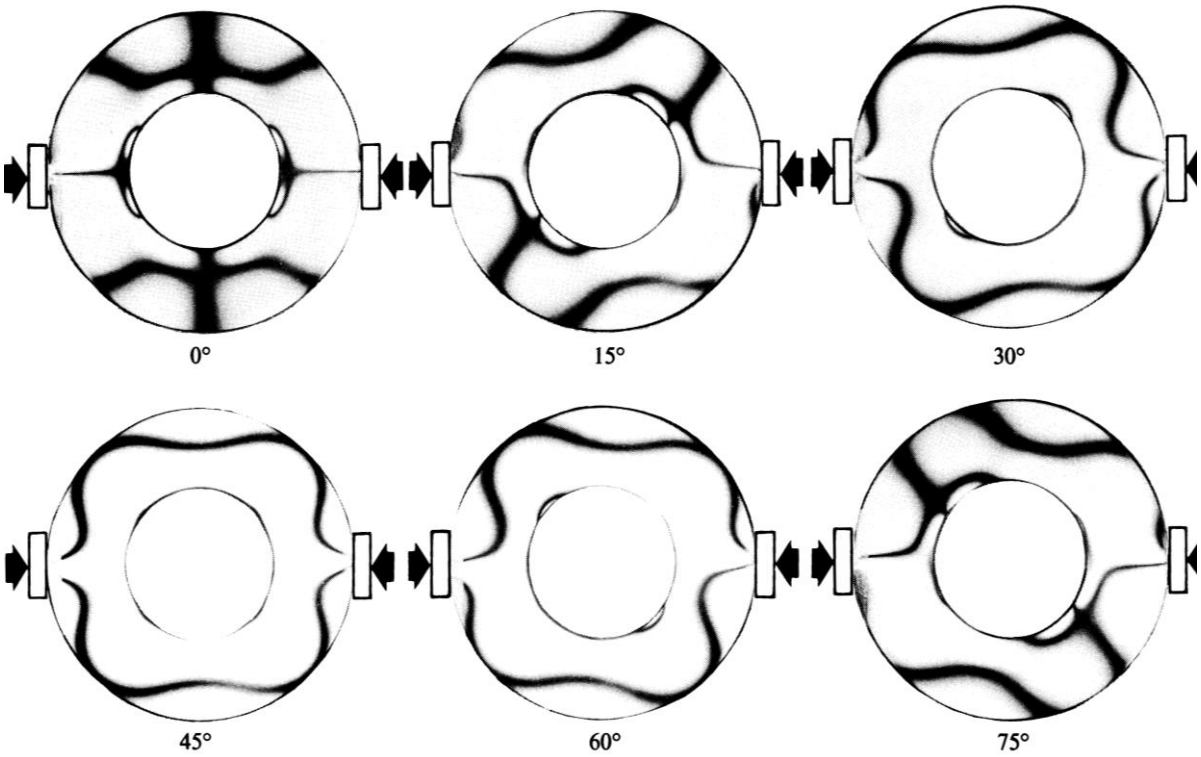

Fig. 3 Isoclinic patterns in a compressed (along diameter) ring

A simple, graphic method may be used for the determination of the principal stress isostatics (trajectories) determination. The first step is the preparation so-called the overall graph of isoclinics (the isoclinic lines registered for different α are combined into a single graph) - (fig. 4a). Then the isostatics can be drawn following the procedure described below:

1) establish the direction of the reference
2) on the isoclinic with parameter α_1 establish point A
3) from this point (A) draw a straight line at the angle $(\alpha_1 + \alpha_2)/2$ to the intersection with the isoclinic line α_2 in the point B
4) repeat step 3) for determination a point C, D … and so on
5) direction of the second principal stress σ_2 is perpendicular to the σ_1

This procedure is presented in fig. 4b.

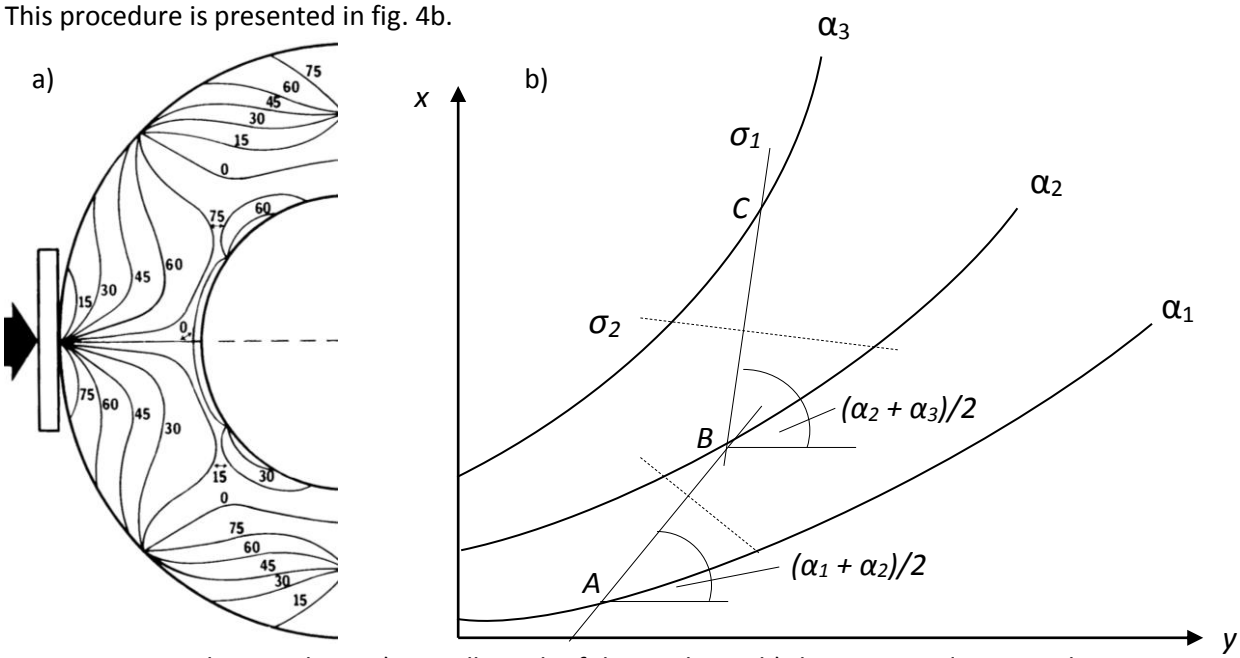

Fig. 4 Isoclinic analysis: a) overall graph of the isoclinics, b) the isostatic drawing scheme

The isostatics illustrate the "flow" lines of principal stresses through the model because they are everywhere tangent to the principal stress directions.

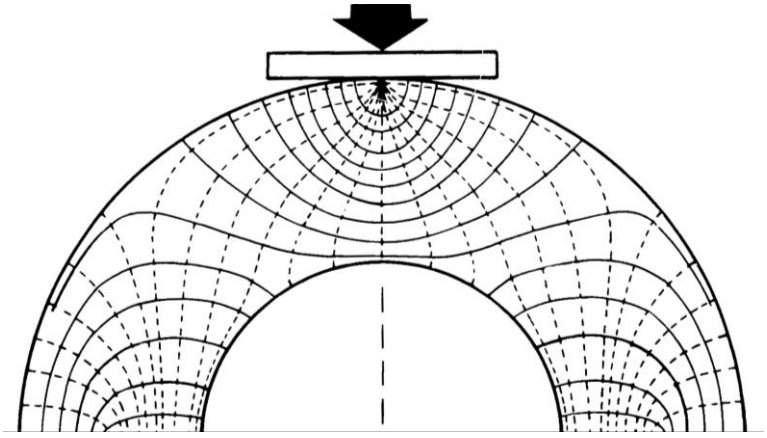

Fig. 5 The isostatic lines obtained for a compressed ring

The photoelastic data, i.e. fringe order N and isoclinic parameter α, inform directly about:

- the difference of the principal stresses $(\sigma_1 - \sigma_2)$ – eq. (3)
- maximum shear stress τ_{max} – eq. (4).

Using the equations (5) it is possible to calculate the difference between the normal stresses $(\sigma_x - \sigma_y)$ and the shear stress τ_{xy}.. Commonly, for the quantitative analysis of the stresses the full-field registration of the isochromatic fringes is used (fig. 6).

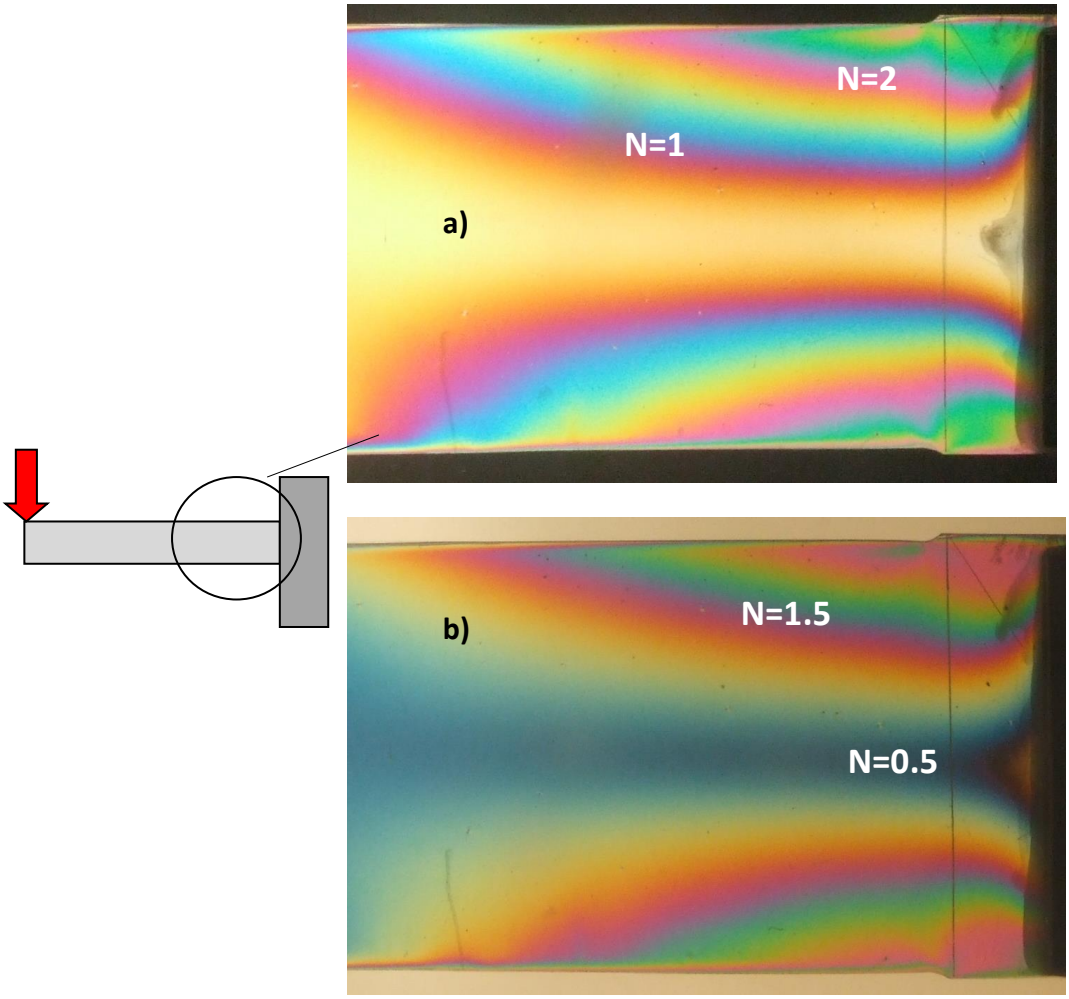

Fig. 6 Isochromatic fringes (a – full-order, b – half-order) in the centilever beam (at the clamped end)

Taking in to the consideration the fact that on the free (not loaded) boundaries of the model the principal stress σ_2 is zero, an other principal stress σ_1 is described by the equation:

$$\sigma_1 = \frac{N f_\sigma}{t} \tag{6}$$

If a pressure with a known value p is acting on the edge of the model, the principal stress σ_1 is calculated with the formula:

$$\sigma_1 = \frac{N f_\sigma}{t} - p \tag{7}$$

For a non-straight edge, described by the function $y = f(x)$, the value of the shear stress τ^b acting in the analyzed point *A* of this edge can be achieved using the formula:

$$\tau^b = -\frac{(\sigma_1 - \sigma_2)}{2t}\sin 2(\alpha_A - \beta) = -\frac{N_A f_\sigma}{2t}\sin 2(\alpha_A - \beta) \tag{8}$$

where β is defined by:

$$\beta = arc\ tan\frac{df}{dx} \tag{9}$$

The individual values of the normal (or principal) stresses at points not located on the free boundaries must be determined using additional experimental data or analytical solutions of the equilibrium equations for plane (biaxial) stress state. In the first case different experimental methods are used (for example interferometry, resistance strain gauges, photoelastic oblique incidence technique). For the analytical separation of stress components, the equations of the equilibrium in the absence of the mass forces are commonly applied:

$$\frac{\partial \sigma_x}{\partial x} + \frac{\partial \tau_{yx}}{\partial y} = 0; \qquad \frac{\partial \sigma_y}{\partial y} + \frac{\partial \tau_{xy}}{\partial x} = 0 \tag{10}$$

An integration of these equations leads to the separated stress components σ_x and σ_y. For example, the integration of the first equation (10) gives:

$$\sigma_x = (\sigma_x)_0 - \int \frac{\partial \tau_{yx}}{\partial y} dx \tag{11}$$

In practise eq. (11) is approximated by the finite-difference expression:

$$(\sigma_x)_i = (\sigma_x)_0 - \sum_0^i \frac{(\Delta \tau_{yx})_i}{\Delta y}\Delta x \tag{12}$$

After the determination of this stress component, the second normal stress σ_{yi} may be calculated using the formula:

$$(\sigma_y)_i = (\sigma_x)_i - (\sigma_1 - \sigma_2)_i \cos 2\alpha_i \tag{13}$$

Basing on the fact that the right sides of the equations (12) and (13) can be easily determined using photoelastic data, the so-called shear-difference method (introduced by M.M. Frocht) is an effective tool for the calculations of the stress components at every point along a chosen line (cross-section) – fig. 7.

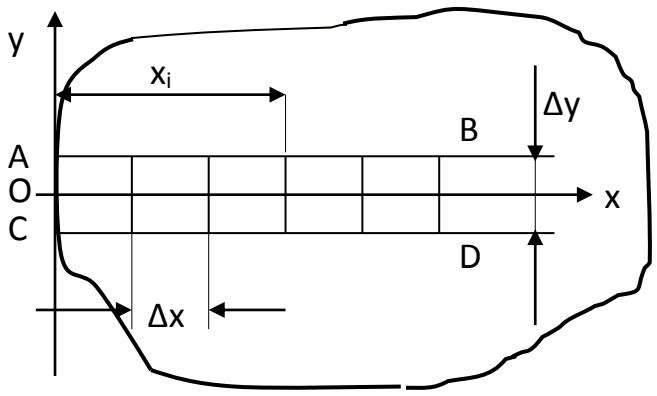

Fig. 7 Scheme of the grid used with the shear-difference method

The first step of the calculations is the determination of the shear difference:

$$\left(\Delta\tau_{yx}\right)_i = \left(\tau_{yx}\right)_i^{AB} - \left(\tau_{yx}\right)_i^{CD} \tag{14}$$

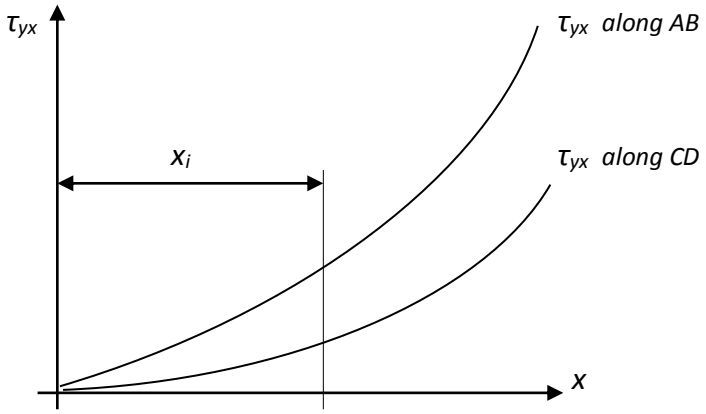

Fig. 8 An example of the τ_{xy} distributions along supporting lines *AB* and *CD*

The values τ_{yx} at every point in the knots of the grid are calculated using the formula:

$$\left(\tau_{yx}\right)_i = \frac{N_i f_\sigma}{2t}\sin 2\alpha_i \tag{15}$$

It is usually accepted that $\Delta x = \Delta y$, so *AB* and *CD* lines are situated at $\pm \Delta y/2$ distance from *Ox* line (analyzed cross-section). For this condition the equation (12) takes the form:

$$\left(\sigma_x\right)_i = \left(\sigma_x\right)_0 - \sum_{i=1}^{i}\left(\Delta\tau_{yx}\right)_i \tag{16}$$

After the determination of the $(\sigma_x)_i$ component, calculations of the second normal stress $(\sigma_y)_i$ are carried out using the formula:

$$\left(\sigma_y\right)_i = \left(\sigma_x\right)_i - N_i\frac{f_\sigma}{t}\cos 2\alpha_i \tag{17}$$

The advantage of the shear-difference method is the possibility to provide calculations along interesting cross-section; for example for a comparison of the obtained results with analytical or numerical (FEM) calculations. The higher accuracy of calculations may be achieved if the N_i and α_i are measured at the grid knots using the compensation techniques.

The components of the plane stress state may also be computed using the Laplace equation:

$$\nabla^2\left(\sigma_x + \sigma_y\right) = 0 \tag{18}$$

A numerical solution of the equation (18), based on the finite-difference form, leads to *n* equations with *n* unknown variables $(\sigma_x + \sigma_y)$ in knots of the orthogonal mesh (fig. 9).

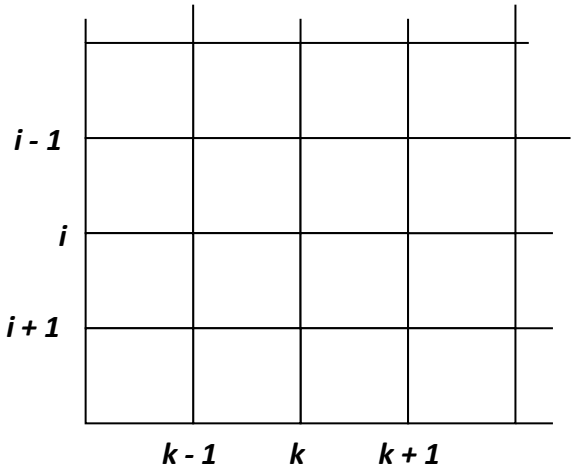

Fig. 9. Mesh for Laplace's equation numerical solution

For every point of the presented mesh the equation has the following form:

$$\frac{(\sigma_x+\sigma_y)_{i+1,k}-2(\sigma_x+\sigma_y)_{i,k}+(\sigma_x+\sigma_y)_{i-1,k}}{\Delta x^2}+\frac{(\sigma_x+\sigma_y)_{i,k+1}-2(\sigma_x+\sigma_y)_{i,k}+(\sigma_x+\sigma_y)_{i,k-1}}{\Delta y^2}=0 \tag{19}$$

For solving this equations system it is necessary to obtain $(\sigma_x + \sigma_y)$ values on the boundary of the analysed region. The second method of the Laplace's equation is an analytic solution by the separation of the variables.

Similarity of the stress field in the model

The photoelastic two-dimensional analysis is connected with the problem of the model's similarity to the original object (prototype). Usually material and dimensions of the model are different from ones of the object. The elastic constants of the materials applying in photoelasticity differ significantly – especially Young's modulus $E^m \ll E^o$. For plane-stress or plane-strain states the stress distributions are usually independent of the elastic constants. It is shown in the stress compatibility equation, which is independent of the Young's modulus:

$$\nabla^2\left(\sigma_x^2+\sigma_y^2\right)=-(1+\nu)\left(\frac{\partial F_x}{\partial x}+\frac{\partial F_y}{\partial y}\right) \tag{20}$$

The Poisson's ratio influence is connected with the mass-forces distribution. For absence of the mass=forces:

$$\left(\partial F_x/\partial x+\partial F_y/\partial y\right)=0 \tag{21}$$

the stress distributions obtained from the photoelastic two-dimensional analysis are independent of this material constant. The same results are obtained for a uniform field of mass-force, i.e. gravitational, or when the mass-force field is changing linearly in *x* and *y* directions.

The equation (20) is not valid for a model with a hole or series of holes when the resultant force applied to the hole's boundary is not zero. In this case the Poissons's ratio influences the stress distributions, but usually less than about 7 %. The second exception of the eq. (20) validity is model's distortion under loading, because this effect causes geometrical changes of the model's shape (for example the geometry of the notches) and load distribution. It may be minimized by a proper selection of the model material, thickness and level of the model loading.

In most two-dimensional photoelastic analysis the similarity of the model and the object tested is described by dimensionless scales (ratios) directly. The scale is defined as:

$$S_i = \frac{x_i^o}{x_i^m} \tag{22}$$

where x_i is a physics quantity, and indices o and m denote original object and model, respectively. Based on Buckingham π theory, the product of the quantity dimensions (describing the analysed phenomenon) must equal one. Thus, the criterion of the similarity, for example for stresses in the body loaded by P force, has the form:

$$C_\sigma = \frac{[\sigma][t][l]}{[P]} = 1 \tag{23}$$

For displacements δ the similarity criterion is:

$$C_\delta = \frac{[\delta][E][t]}{[P]} = 1 \tag{24}$$

Introducing scales and rewriting (23) and (24), the stresses and displacements in the prototype are:

$$\sigma^o = \sigma^m \frac{P^o}{P^m} \frac{t^m}{t^o} \frac{l^m}{l^o} \tag{25}$$

and

$$\delta^o = \delta^m \frac{P^o}{P^m} \frac{t^m}{t^o} \frac{E^m}{E^o} \tag{26}$$

Of course, the model should be loaded in the same scheme of loading as the original object and the geometry (shape) must be identical in the linear dimensions scale ($S_l = l^o/l^m$). In two-dimensional photoelastic analysis the scale of the thickness is often different from linear dimensions scale. This difference may be easily taken in to consideration basing on the equations (25) and (26).

Model's material calibration

For the quantitative analysis of the photoelastic data, the material fringe value f_σ must be determined. This "constant" varies with the type of birefringence materials, curing technology, temperature, time and so on. Thus it is necessary to calibrate each model material close to the time of the experiment.

The principle of the calibration is simple: it must be realised on the sample for which the theoretical stress distribution is known. This sample is loaded with a known loading path and isochromatic fringes at several levels of the load are registered. Then the comparison of the stress value and isochromatic fringe existing in the same point enables to determine the f_σ value.

The most popular samples for material fringe value determination are a four-point bending beam and a circular disc compressed along its diameter. In the first case the sample with the rectangular cross-section is subjected to bending according the scheme presented below.

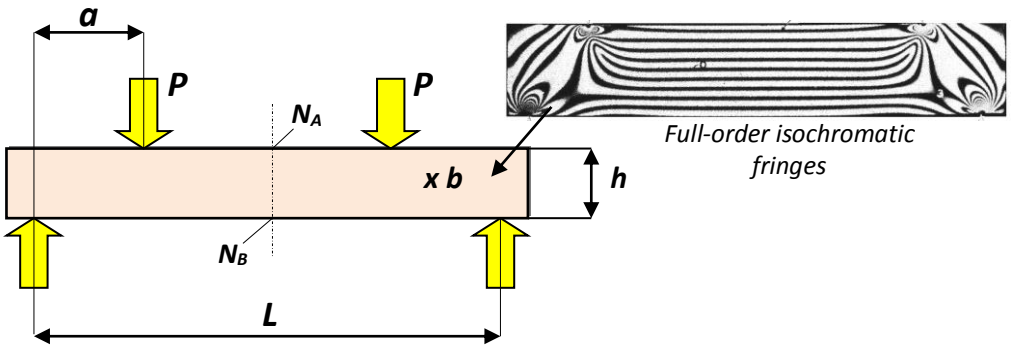

Fig. 10 Scheme of the four-beam bending calibration

The fringe order value f_σ is calculated based on the formula:

$$f_\sigma = \frac{6Pa}{N_{av}h^2}; \qquad N_{av} = \frac{N_A + N_B}{2} \tag{27}$$

The second popular sample is a compressed circular disc (fig. 11).

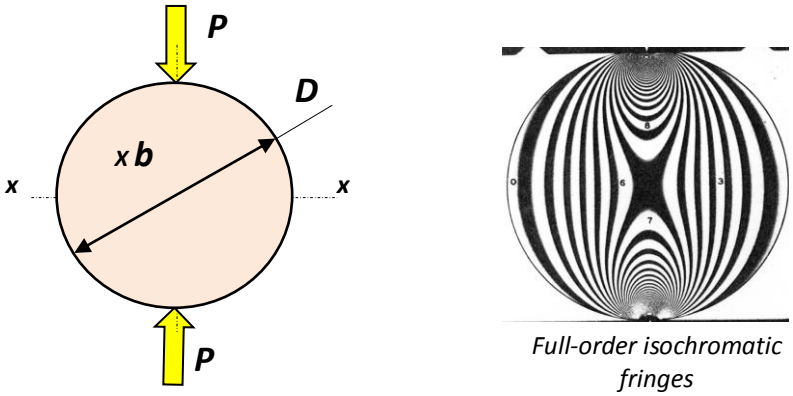

Fig. 11 Scheme of the compressed disc calibration

The principal stresses difference along the horizontal *(x-x)* diameter of the sample is:

$$f_\sigma = \frac{8P}{\pi ND}\left[\frac{D^4 - 4D^2x^2}{(D^2 + 4x^2)^2}\right] \tag{28}$$

In practise the fringe order is measured in the central point of the disc (often using compensation technique of the fringe order determination) and the equation (28) reduces to:

$$f_\sigma = \frac{8P}{\pi ND} \tag{28a}$$

The calibration of sample's thickness is commonly $b = 10$ mm and f_σ obtained for such samples is called the material fringe order value. If the tested model has different thickness $t \neq b$ the model fringe order value $f_{\sigma m}$ may be calculated:

$$f_{\sigma m} = \frac{f_\sigma}{t} \tag{29}$$

In such cases the equation (3) – basic relationship for two-dimensional photoelastic analysis – has the form:

$$(\sigma_1 - \sigma_2) = N f_{\sigma m} \tag{30}$$

Model materials

The selection of the model materials is of a great importance the for results of the photoelastic analysis. The essential features of these materials should be:

- high sensitivity, i.e. a low level of loading causes high fringe order
- linear characteristics: stress difference vs. isochromatic fringe order, stress vs. strain
- isotropy and homogenity: mechanical and optical
- low temperature influence on the material properties
- excellent transparency
- good machinability
- low time-edge effect, caused by diffusion of the water vapour from/or in the model material, producing additional optical effects (isochromatic fringes) mainly at the model edges.

The two-dimensional models are prepared by machining from the sheets (of different thickness) produced by casting – fig 12.

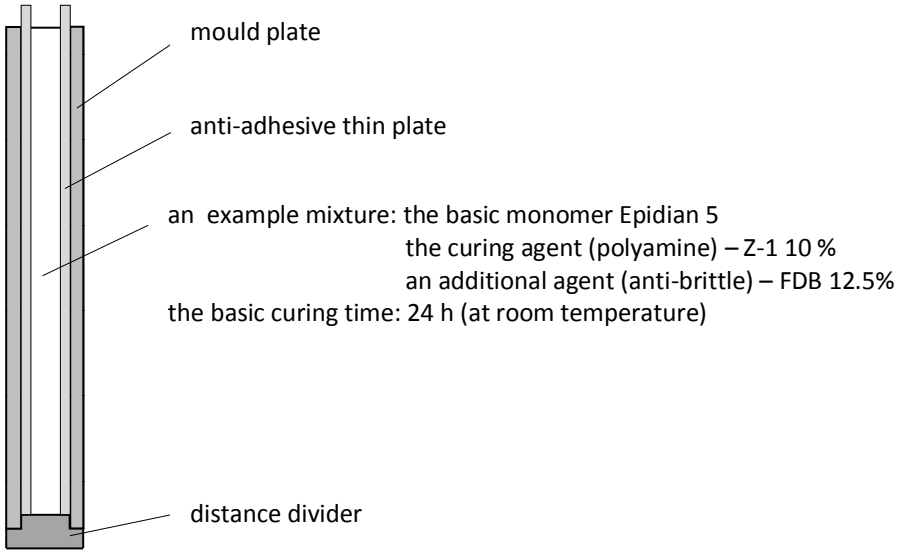

Fig. 12 Scheme of the mould for sheet casting

The main requirement of the cutting, drilling and other machining processes during the model preparation is avoiding of generation of the heat produced by the forces acting on the plastics during model shape forming. This heat effect produces “non-removable” high order isochromatic

fringes at the edges. Actually, the abrasive water jet technique is more often used. Approximate basic characteristics of the several types of the model materials are presented in table 1.

Properties of the model materials (approx.)

Table 1.

Material	***E*** [MPa]	***ν*** [-]	σ_{prop} [MPa]	$f_{\sigma} x 10^{-2}$ [MPa/m fr.ord.]
glass	68 300	0.22	29.4	20 - 30
epoxy resins				
Araldit D	3 600	0.36	20.6	1.30
Epidian 5	3 200	0.36	20.0	1.25
polyester resins	4 000	0.36	-	2.50
PMMA	3 400	0.36	19.6	26
polycarbonate	2 500	0.38	34.5	0.73
urethane rubber	3	0.46	0.14	0.018
gelatine	0.02	-	-	0.029

Example of the analysis

One of the most simple problems of the two-dimensional stress state analysis, often solved experimentally, is determining the stress concentration factor. The stress concentration is a well known effect observed at the holes and notches or other geometrical irregularities, which is characterised by a high gradient of the stresses components on the small distance from the concentration source. This factor is defined by:

$$\alpha = \frac{\sigma_{max}}{\sigma_{nom}} \tag{31}$$

As a rule, σ_{max} is the maximum value of the stress component on the non-loaded edge of the irregularity in the tested model, and σ_{nom} is the stress value of the same component calculated for a body without an irregularity. The stress concentration causes specific isochromatic fringes distributions – fig. 13 (highest isochromatic fringe order on the notch edge, a significantly higher gradient of *N* at the notch corner).

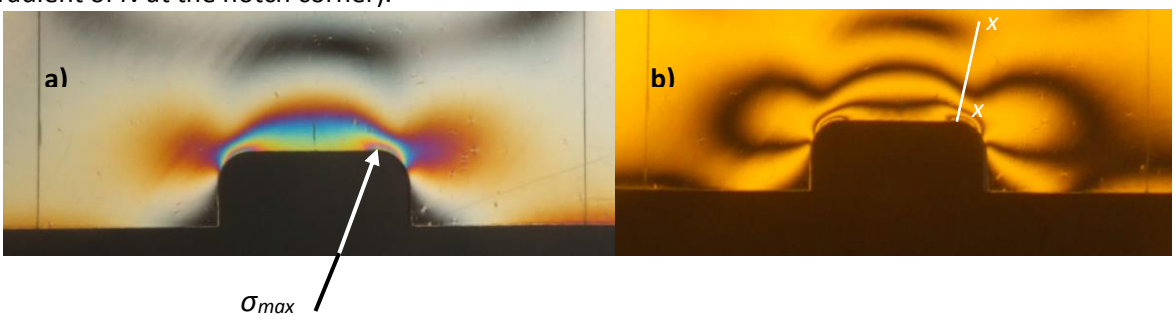

Fig. 13 The full-order isochromatic fringes around a notch (in bended cantilever beam): a) white light beam, b) monochromatic (sodium) light

The maximum Isochromatic fringe order N_{max} is determined by an extrapolation of $N(x)$ function along the line situated perpendicularly to the edge (line x-x) and the equation (30) is used for σ_{max} calculation. The nominal stress is calculated using a well known relationships, for example for bending cantilever beam without a notch for cross-section defined by the localization of x-x line. The same analysis can be carried out for a tensile strip with a circular hole – fig. 14.

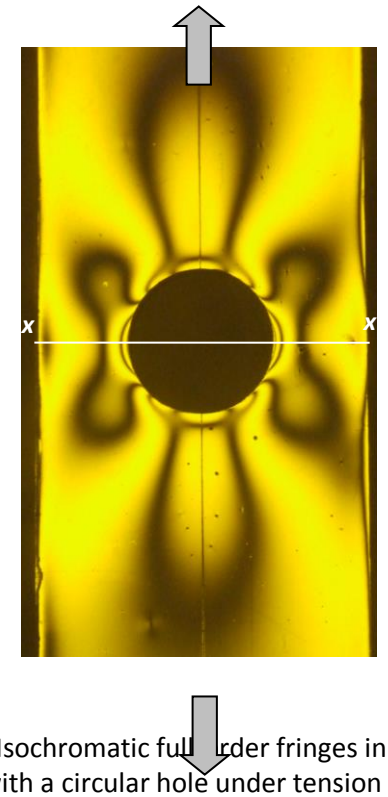

Fig. 14 Isochromatic fu[illegible]rder fringes in the strip with a circular hole under tension loading

In this case the maximum stress σ_y existing on the hole edge in the x–x cross−section and determination of the $N(x)$ allows for the σ_{max} calculation. For the σ_{nom} calculation the stress state in the strip without a hole must be considered and its value is:

$$\sigma_{nom} = \frac{P}{bt} \tag{32}$$

The more detailed analysis of the stress distribution around the hole, the analytical solution of the Kirsch's problem must be used, i. e. the thin plate with infinite in-plane dimensions and a circular hole (with diameter 2R) under tension - fig. 15. The uniform stress field with σ_0 value exists in y direction at the polar coordinate $r \to \infty$. The boundary conditions are:

$$\sigma_y = \sigma_0 \qquad r \to \infty, \quad \sigma_r = \tau_{r\theta} = 0 \qquad r = R, \quad \sigma_x = \tau_{xy} = 0 \qquad r \to \infty$$

Using the Airy's stress-function for stress field representation, the stress components at any point in the plate with the coordinate r, Θ are:

$$\sigma_r = \frac{\sigma_0}{2}\left\{\left(1 - \frac{R^2}{r^2}\right)\left[1 + \left(\frac{3R^2}{r^2} - 1\right)\cos 2\theta\right]\right\} \tag{33a}$$

$$\sigma_\theta = \frac{\sigma_0}{2}\left[\left(1+\frac{R^2}{r^2}\right)+\left(1+\frac{3R^4}{r^4}\right)\cos 2\theta\right] \quad (33b)$$

$$\tau_{r\theta} = \frac{\sigma_0}{2}\left[\left(1+\frac{3R^2}{r^2}\right)\left(1-\frac{R^2}{r^2}\right)\sin 2\theta\right] \quad (33c)$$

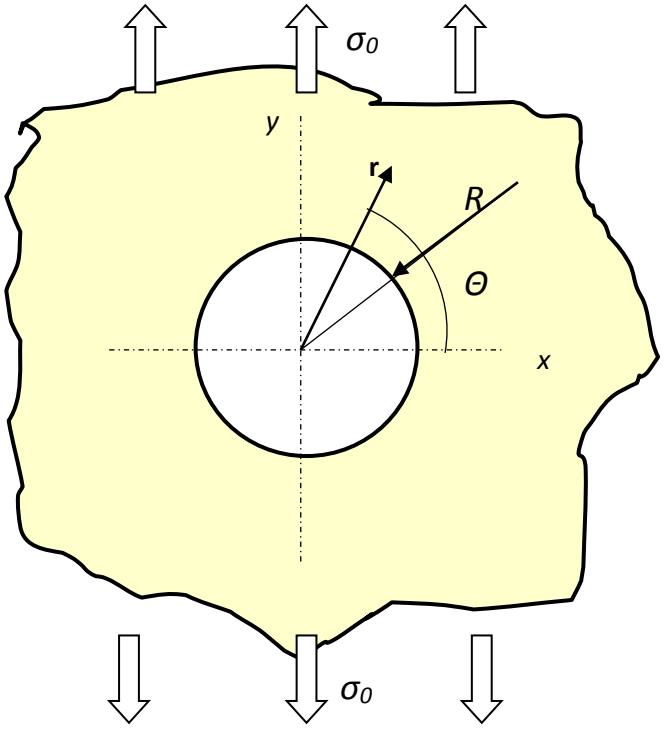

Fig. 15 The infinite plate with a circular hole subjected to the axial tension load

The most interesting phenomenon is the stress distribution along the x axis. For $\Theta = 0$ and $r = x$ equations (33) have the forms:

$$\sigma_x = \frac{\sigma_0}{2}\left(1-\frac{R^2}{x^2}\right)\frac{3R^2}{x^2}; \qquad \sigma_y = \frac{\sigma_0}{2}\left(2+\frac{R^2}{x^2}+\frac{3R^4}{x^4}\right); \qquad \tau_{xy} = 0 \quad (34)$$

It must be noted that these equations are valid for an infinite plate. If the plate has the finite dimensions (for example width), this fact influences the stress distributions. For the tension strip there can be observed a non-uniform stress distribution along the edges parallel to the *y* axis (see fig. 14) in the proximity of the hole and σ_{ymax} (for $\Theta = 0$) not equal 3.0 (this value is obtained for infinite plate).

The towing hitch – several remarks

A *tow hitch* (*tow bar*) is a device attached to the chassis of a vehicle for towing the trailers (luggage t., camp t., cattle t.). In the European Union the tow bars must be approved to the European Union directive 94/20/EC to be fitted to vehicles first registered on or after 1 August 1998. They are standardized according to the ISO standard BS ISO 1103:2007. The ISO tow-ball is 50 mm in diameter and has been accepted in most of the countries except North America. The basic categories of ISO

tow-ball are: the flange fitting and the swan-neck (fig. 16) which has an extended neck fitting into the tow-bracket. Swan-neck tow-balls are often removable.

Fig. 16 Categories of the tow-ball: flange fitting (above) and swan-neck type (below)

The main loading forces determining the tow hitch capacity are (fig. 17):

- *tongue weight (TW)* - the force acting downward exerted on the ball by the trailer coupler
- *gross towing weight (GTW)* - the weight of the trailer with the cargo in it (fully loaded trailer)

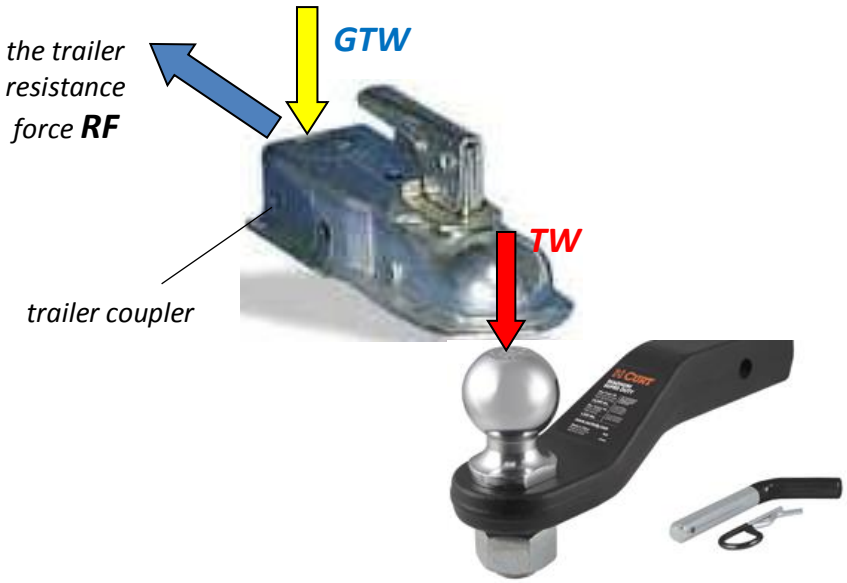

Fig. 17 Tow hitch loading scheme

The resistance force of the trailer movement (for constant velocity $v = 0$ and trailer tongue parallel to the road surface -fig. 18) is the sum of trailer's rolling force $F_{r,t}$, aerodynamic resistance force F_{at} and hill resistance force F_{ht} (eq. 35).

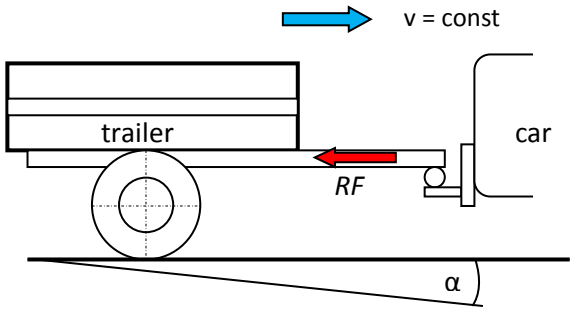

$$RF = F_{rt} + F_{at} + F_{ht} \tag{35}$$

$$F_{rt} = (GTW) f_t \cos\alpha \tag{35a}$$

$$F_{at} = (0.1 \div 0.3) F_a \tag{35b}$$

$$F_{at} = (0.1 \div 0.3) F_a + c_{xt} A_t \rho \frac{v^2}{2} \tag{35c}$$

$$F_{ht} = (GTW) \cos\alpha \tag{35d}$$

where: f_t – rolling resistance coefficient, F_a – aerodynamic resistance force of the car, c_{xt} – trailer drag coefficient, ρ – air density, A_t – trailer's cross-section area over the cross-section area A_c of the car.

The equation (35c) is used for towing a trailer with a larger cross-section area than a car. The box-shape trailers have the drag coefficient c_{xt} = 1.0 – 1.3.

Practical tasks

During practical exercises the following activities will be carried out:

- presentation of practical information about the technology of plain (2D) models preparation, and demonstration of different objects models,
- exercises in isoclinics and isochromatics recognition, using a Carl-Zeiss Jena polariscope,
- calculation of the similarity scale
- performing a photoelastic measurement: determination of fringe order value f_σ, registration of full- and half-order isochromatic images, calculation of strains/stresses in a chosen cross-section of the model under investigation
- preparation a report (its range will be determined by the lecturer).

References

[1] Dally J.W., Riley W.F., Experimental Stress Analysis (3rd ed.), McGraw-Hill, Inc., 1991.
[2] Measurements Group Tech Note, (polariscope producer's technical references), 1989.
[3] Kobayashi Alberts (ed.), Handbook on Experimental Mechanics, Englewood Cliffs, NJ, Prentice-Hall, Inc., 1987.

[4] Sharpe, Jr., Wiliam N. (ed.), Springer Handbook of Experimental Solid Mechanics, 2008.
[5] Ellis J.R., Vehicle Dynamics, London Business Books, 1969
[6] Photoelasticity (laboratory instruction – in polish), http://riad.usk.pk.edu.pl/~biomech/laboratoria/druki/w9.pdf